International Research Journal of Engineering and Technology (IRJET) e-ISSN: 2395-0056
Volume: 08 Issue: 04 | Apr 2021 www.irjet.net p-ISSN: 2395-0072

Thermal Performance Analysis of Greenhouse Solar Dryers using Computational Fluid Dynamics and Comparison with Different Geometrical Structures

Kushagra Chawda[1], Tanmay Khare[2]

[1,2]*Jabalur Engineering College, Jabalpur India*

Abstract - *The computational fluid dynamics of a greenhouse solar dryer is undertaken which reveals the variations in physical properties of moist air, which is the heat carrying medium inside the greenhouse. The simulation is found to be in agreement with the physical data. K-e model is used to account for the turbulent air flow. Discrete ordinate radiation model is also employed, since the heat transfer is also radiative. The parameters used to analyse the performance of the greenhouse solar dryer are air temperature, turbulent kinetic energy and air velocity. The contours of these parameters are also obtained to clearly state the variations. Similar procedures are applied to two other models, namely cylindrical roof and prismatic greenhouses. Consecutively, comparisons and similarities are drawn among the different models and their characteristics. The variations are used to optimize the drying process as per specific needs and cases. The maximum average temperature is obtained in the cylindrical roof Greenhouse - 321 K. Maximum average turbulent kinetic energy is obtained in The chapel type dryer - 0.012 m^2/s^2. Maximum average air velocity is found in Cylindrical roof greenhouse dryer - 0.07 m/s. The variations among different structural geometries are used to optimize the drying process as per specific needs and cases*.

Key Words: Greenhouse dryer, CFD analysis, Turbulent kinetic energy, Greenhouse models, Catia, ANSYS.

1. INTRODUCTION

Drying is the process of preserving food products to be used for more extended periods. The concept of using sun rays accompanied by the winds is not new. The technique has been around for long. One of the oldest preservation techniques for food products has been drying. The reduction in the moisture content of the food product, as a consequence, makes it lighter and thus easier to carry and store. However, interestingly, the nutritional content remains intact during the process of drying. Furthermore, the process of drying also represses the growth of bacteria, yeast, and mold. So, the food becomes even more suitable for consumption.

Many food items are dehydrated, including fruits like apples, peaches, and apricots to make fruit chips, cherries, and blueberries for nutrition bars—vegetables like onions, peas, carrots for adding in soups and other dishes. Meat products like beef jerky and dehydrated fish like sardines are top-rated. Herbs like oregano, basil, and rosemary are dry to elongate their shelf lives.

It can be easily observed that the most rudimentary drying technique - sun-drying has its cons that outweigh the pros[1]. Although it is a better process than using fossil fuels that are costly and harmful to the environment, better alternatives like greenhouse solar dryers exist. The use of solar energy provides a cheaper and environment-friendly operation. This advanced method is being researched and modified by accompanying several fixtures that provide wind convection variations to optimize the outcomes.

Two major types can be identified among the various types of solar dryers being worked upon and used. The primary difference in them is the type of convection provided - namely forced convection or natural convection. As suggested by their names, natural convection of air is established by buoyancy-induced airflow in natural convection and contrastingly forced convection dryers to employ external powered fans. This research paper deals with natural air convection provided by air inlets. However, a constant airflow is difficult to maintain with only wild winds. To counter this issue, ventilators are sometimes installed at the outlets.

Temperature is one of the most crucial factors in developing biological processes involved in the drying process[2]. According to the research done in the field, the uniformity of crop growth is also significantly affected by temperature distribution. The correlations between the distribution of pests and temperature distribution have also been observed[3]. Therefore, the initial focus of this study has been temperature distribution.

With computational software like ANSYS and Catia, the study of Greenhouse solar dryers becomes quite lucid. The computational fluid dynamics models can simulate the wind and heat flow process that would have been difficult and cumbersome to note with the sensors. It can also isolate areas for further analysis and study. The study of the simulations and its analysis, followed by practicing the

findings, in reality, will reduce the drying process and cost reduction involved with the installation of dryers.

Among other noteworthy studies, the computational analysis of a greenhouse environment as a controlled system to come up with ways to improve the harvesting levels[4]] further reinforce the positive outcomes from such studies. The basic skeleton of using a modeled space with constant heating and convection induced by inlet-outlet system ventilation is noted. The analysis is completed with the help of a standard k-epsilon model to acknowledge turbulent transport phenomena. The results are plotted in terms of temperature, velocity, and pressure readings.

A similar study was undertaken by a team of researchers from Mexico[5], further identifies the shortcomings of previous studies done in the field and attempts to enhance and optimize the computational process while taking into account the relations of the system with Thermal Kinetic Energy. Thermal Kinetic Energy is the mean parameter for the observed leading homogeneity of air temperatures in greenhouse solar dryers. That study involved two greenhouse solar dryers of the chapel shape. The minute difference between the two is a change in height. The team also used an actual greenhouse dryer to correlate the modeled system's findings with precise temperature and air velocity changes. The results have similarities to a considerable extent. The analysis had been done via ANSYS FLUENT.

Our research intends to build up further on using different solar greenhouse dryers structures and analyze the differences obtained in terms of temperature, thermal kinetic energy, and air velocities. While using the Mexican team's boundary conditions[5], four types of geometries have been studied. The first being the usual chapel type, secondly a cylindrical rooftop, and lastly, a conical camp type shape.

The dimensions of all the four structures have been kept as close to possible, and the mimicking of the boundary conditions is done to ensure uniformity which might be otherwise difficult to obtain in the real world, but for the sake of the immediate comparison purposes, turn out to be a necessity. The analysis models follow the broadly accepted k -epsilon model of the ANSYS FLUENT.

2. MATERIALS AND METHODS

2.1 Experimentation and Setup

A chapel-type greenhouse installation setup in Mexico is used as a paradigm[5]. There are two inlet ports and two outlet ports that provide convection of air inside the greenhouse dryer. A constant airflow is maintained, making the installation to be a forced convection type greenhouse solar dryer. Physical measurement on the project site included readings of the following:

Solar radiation
Inside air temperature
External air temperature
Air velocity

The choice of the above-mentioned experimental setup is majorly dependent on the Mexican team's appreciable similitude between the physical parameter readings and the computational observations. Minimal errors and differences could be very well accounted to the sensors' sensitivity since they were within a range of 1 Kelvin.

The boundary conditions in that geometrical model are being used to predict different structures other than the chapel type. Keeping the material constant and the convection similar, we can compare different designs. Although the readings cannot be expected to be the same in other places geographically and during the year, it makes sense to use a single set of readings and boundary conditions for all the models. This process is sufficient for carrying out analogical deductions.

2.2 Computational Analysis

The scalar and vector fields within the greenhouse can be evaluated by the CFD analysis, which simulates the ventilation's air transport equations[6]. As discussed earlier the convection provided by ventilation is responsible for the heat transfer taking place.

The boundary conditions of the greenhouse gas walls, which are assumed to have a constant uniform temperature, are discussed in Table 1. The floor is taken to be an adiabatic entity. The properties of air as a transfer medium are elaborated in Table 2. The boundary conditions of the material and convectional ventilators are noted down in Table 3.

Table -1: Average wall temperatures

Temperature [K]			
North wall	South wall	West wall	East wall
305.4	310.0	308.6	311.9

Table -2: Properties of moist air

Properties	Unit	Value
Density	kg/m^3	1.0885
Specific heat	J/kg.K	1045.887
Thermal	W/m.K	0.0279

Conductivity		
Dynamic viscosity	Pa.s	1.978 x 10^{-5}

2.3 Mathematical Model

Navier-Stokes theorem is employed to obtain the equations of mass, energy, and momentum. The flow of heat transfer medium air is assumed to be in a steady-state fluid flow, incompressible and turbulent.[11]

Mass conservation equation

$$\nabla\ (\rho v) = 0\ 1$$

Momentum conservation equation:

$$\nabla \cdot (\rho vv) = \nabla\ (\mu \nabla v) - \nabla P + \rho g\ 2$$

Energy conservation equation:

$$\nabla \cdot (\rho vT) = \nabla \left(\frac{\lambda}{C_p} . \nabla T\right) + \Psi\ 3$$

The effect of turbulence on the airflow was implemented via the k-e model, which is a semi-empirical model based on transport equations for the TKE and turbulent dissipation rate (TDR). It is suitable for the analysis of turbulent flows in large spaces[10].

Turbulent Kinetic Energy:

$$\frac{\partial}{\partial x_i}(\rho k v_i) = \frac{\partial}{\partial x_j}\left[(\mu + \frac{\mu_t}{\sigma_k})\frac{\partial k}{\partial x_j}\right] + P_k + P_b - \sigma\varepsilon - Y_M + S_k\ 4$$

Turbulent Dissipation rate:

$$\frac{\partial}{\partial x_i}(\sigma\varepsilon v_i) = \frac{\partial}{\partial x_j}\left[\left(\mu + \frac{\mu_t}{\sigma_\varepsilon}\right)\frac{\partial \varepsilon}{\partial x_j}\right] + \rho C_1 S_\varepsilon - \rho C_2 \left(\frac{\varepsilon^2}{k + \sqrt{v\varepsilon}}\right) + C_{1\varepsilon}\frac{\varepsilon}{k} C_{3\varepsilon} P_b + S_\varepsilon\ 5$$

In the equation (4) and (5), x_j is the 3D coordinate systems, P_k represents the generation of TKE due to the average velocity gradients; P_b is the generation of TKE due to buoyancy; Y_M is the fluctuating dilation incompressible turbulence, and S_k and $S\varepsilon$ are root definitions. The coefficients are included in this model and can be defined as shown below[9].

$C_1\varepsilon$=1.44;C_2=1.9;σ_k=1.0;σ_ε=1.2

$$C_1 = \max[0.43, \frac{\eta}{\eta + 5}]$$

$$\eta = S\frac{k}{\varepsilon},$$

Where $S = \sqrt{2S_{ij}S_{ij}}$

in the turbulent viscosity, we have

$$\mu_t = \rho\mu_\mu \frac{k^2}{\varepsilon}$$

$$C_t = \frac{1}{A_0 + A_S\frac{kU^*}{\varepsilon}}$$

$$U^* = \sqrt{S_{ij}S_{ij} + \tilde{\Omega}_{ij}\tilde{\Omega}_{ij}}$$

$$\tilde{\Omega}_{ij} = \Omega_{ij} - 2\varepsilon_{ijk}\omega_k$$

$$\Omega_{ij} = \bar{\Omega}_{ij} - \varepsilon_{ijk}\omega_k$$

Where $\bar{\Omega}_{ij}$ is the tensor of the center of rotation of speed in a rotating zone with angular velocity ω_k. They have constants A_0 and A_s that described by [9]

$$A_0 = 4.04$$

$$A_s = \sqrt{6}\cos\phi$$

where $\phi = \frac{1}{3}\cos^{-1}(\sqrt{6}W)$

$$W = \frac{S_{ij}S_{ik}S_{ki}}{\tilde{S}^3}$$

$$\tilde{S} = \sqrt{S_{ij}S_{ij}}$$

$$S_{ij} = \frac{1}{2}\left(\frac{\partial u_j}{\partial x_i} + \frac{\partial u_i}{\partial u_j}\right)$$

The DO model allows you to include the effect of a discrete second phase of particulates on radiation. In this case, **ANSYS FLUENT** will neglect all other sources of scattering in the gas phase.[8] It is used to simulate the effect of solar incident irradiance on the greenhouse solar dryer. The semi-transparent walls of polyethylene can be

Table -3: Boundary Conditions

Location	Material	Condition	Parameters	Value
Upper Wall	Polyethylene	Mixed (semi transparent)	Direct irradiance [W/m²] Diffuse irradiance [W/m²] Emissivity Absorption coefficient [1/m] CHT coefficient of external air [W/m² K]	761.05 62.21 0.9 1132 7.497
South wall North wall East wall West wall	Polyethylene	Thermal	Temperature[K]	310.05 305.48 311.98 308.60
Diffuser 1 (west)	Moist air	Inlet	Temperature [K] Mass flow rate [kg/s] TKE [m²/s²] TDR [m²/s³]	323.53 0.2712 0.00118 0.000818
		Outlet	Pressure [Pa] Backflow TKE [m²/s²] Backflow TDR [m²/s³]	87587.76 0.0014 0.00041
Diffuser 2 (east)	Moist air	Inlet	Temperature [K] Mass flow rate [kg/s] TKE [m²/s²] TDR [m²/s³]	323.37 0.2247 0.00164 0.0003
		Outlet	Pressure [Pa] Backflow TKE [m²/s²] Backflow TDR [m²/s³]	87587.76 0.0014 0.00041

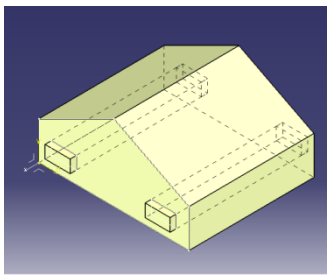
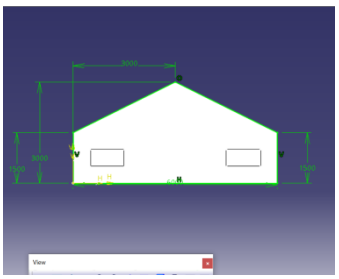
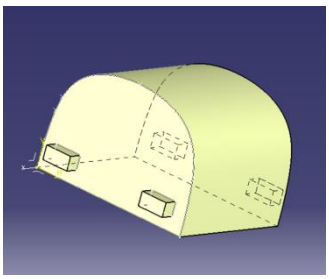
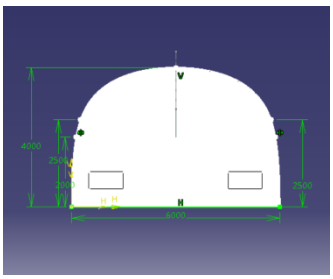

FIGURE 1 Chapel type greenhouse **FIGURE 2** Cylindrical roof greenhouse

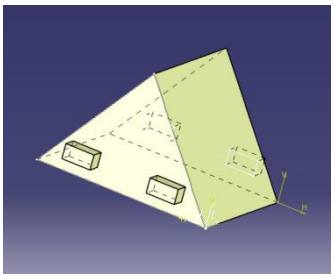
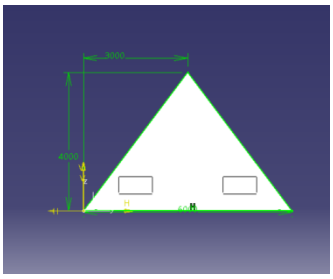

FIGURE 3 Prismatic greenhouse

appropriately solved using this model. The energy equations coupled with the radiation are presented below:

$$\sum_{j=1}^{N} \mu_{ij}^{T} T_j - \beta_i^T - \alpha_i^T \sum_{K=1}^{L} I_i^K \omega_k - S_i^T S_i^h \; 10$$

where
$\alpha_i^T = \kappa \Delta V_i$
$\beta_i^T = 16\kappa\sigma T_i^{*3} \Delta V_i$
$S_i^T = 12\kappa\sigma T_i^{*4} V_i$

where ΔV is the control volume, S_i^h is the source term, and μ_{ij}^T is the coefficient due to convection and diffusion. S_i^h and μ_{ij}^T are evaluated based on the approximate results of the diffusion and convection and the nonradiative terms of the source.

2.4 Structure Modelling

Catia and fusion360 were used for the construction of the four geometries understudy for different structures. The geometries were later imported on the ANSYS software. The three-dimensional software models are made to become an actual image for the space inside the greenhouse, simulated to be made up of moist air.

Meshing of the models was undertaken in ANSYS. A fine meshing was created for the best results. No failures were observed in the meshing. It can also be observed that the quality control factors (orthogonality) of the selected mesh are within a good range[9].

Table -4: Meshing statistics

Geometry	Nodes	Elements
Chapel type	29712	153513
Cylindrical roof	29397	152390
Prismatic	21351	108514

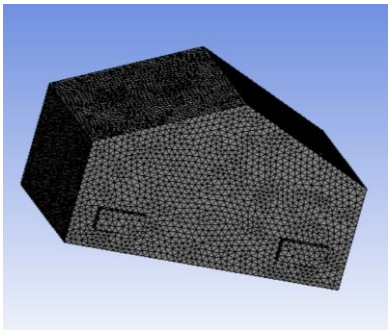

Fig -4: Chapel type greenhouse

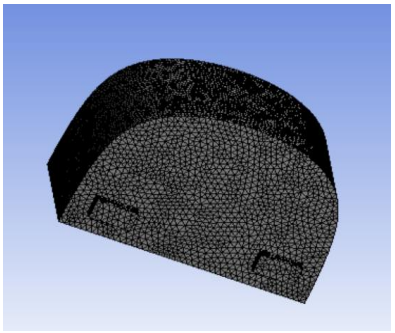

Fig -5: Cylindrical roof greenhouse

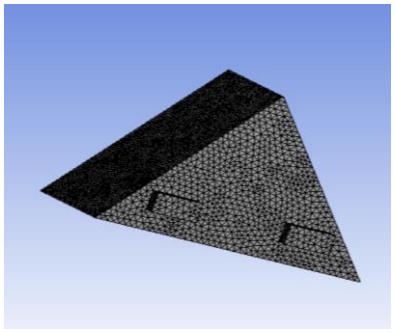

Fig -6: Prismatic greenhouse

2.5 Simulation Procedure

Computational fluid dynamic analysis of the greenhouse solar dryer is undertaken on the ANSYS FLUENT 18.0 software. The models used are energy, radiation DO, and k-epsilon turbulent models. The medium is assumed to be steady-state and turbulent. The SIMPLE algorithm is used for pressure-velocity coupling, and the first-order upwind scheme is used to discretize the convective terms in the momentum, energy, and turbulence equations.

The structures are divided into three sections longitudinally and three sections transversely to study the greenhouse effect parameters. Figures 7-9 explain these sections. Temperature, air velocity, and turbulent kinetic energy plots are obtained in these sections for each of the four geometries. A constant distance of 2 m is maintained between these sections.

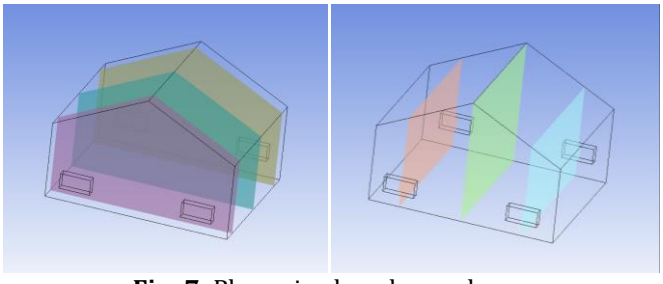

Fig -7: Planes in chapel greenhouse

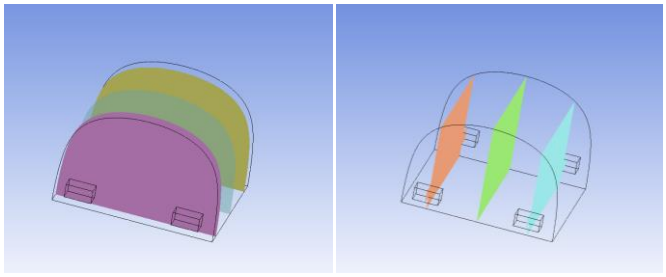

Fig -8: Planes in cylindrical greenhouse

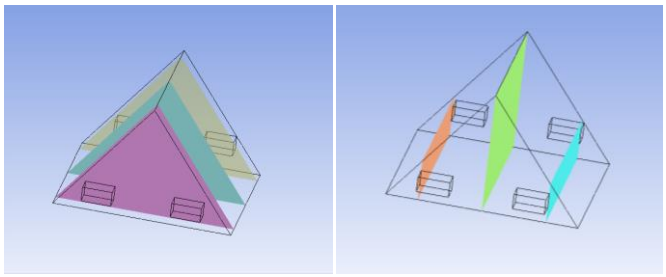

Fig -9: Planes in prismatic greenhouse

3. RESULTS AND DISCUSSION

The controlled space inside the greenhouse solar dryer is observed to be heterogeneous, where different regions have different readings of temperature and other parameters. The values of the physical properties are plotted on the planes mentioned in the previous section. The three main parameters of comparison are air temperature, air velocity, and thermal kinetic energy. The planes' names correspond to the plane colors from Figures 7-9, as displayed in the following index.

Table -4: Longitudinal Plane nomenclature

Plane display color	Plane name
Pink	Plane A
Blue	Plane B
Yellow	Plane C

Table -5: Transverse Plane nomenclature

Plane display color	Plane name
Orange	Plane D
Green	Plane E
Blue	Plane F

3.1 Air temperature Results

The air temperature graphs for different greenhouses are shown in Figures 10-12. Across the angular models, it is observed that as the warm air enters the greenhouse from the inlet ports and it cools down rapidly as it passes through the length of the structure. The contours near the planes D and F are very similar, but the temperature in the central zone is mainly homogeneous, attributed to the effect of thermal Kinetic Energy produced due to the solar irradiance. Whereas in the curvilinear model, namely, the cylindrical roof greenhouse cannot provide a homogeneous distribution of temperatures. The warm air passage can be identified by connecting the inlet valves to the outlet valves.

The growth of crops is greatly affected by the temperature, and so is the drying process. Continuing the line as mentioned above of thought, it can be stated that racks and height-wise distribution in cylindrical roof greenhouses might lead to non-uniform results. That said, the average temperatures were the highest for the cylindrical roof greenhouse, being 321K as opposed to 314 and 317.5 for the chapel type and the prismatic greenhouse, respectively. This becomes important for judging the types of crops to be processed in optimum and minimum temperatures[13].

3.2 Turbulence Kinetic Energy Results

The turbulence kinetic energy inside the greenhouse dryer has an intense correlation to the inlet and outlet valves' forced convection. The contours of TKE distribution in the different models are shown in figures 13-15. The outlines are primarily homogeneous, with specific concentrations near the valves. This is due to the

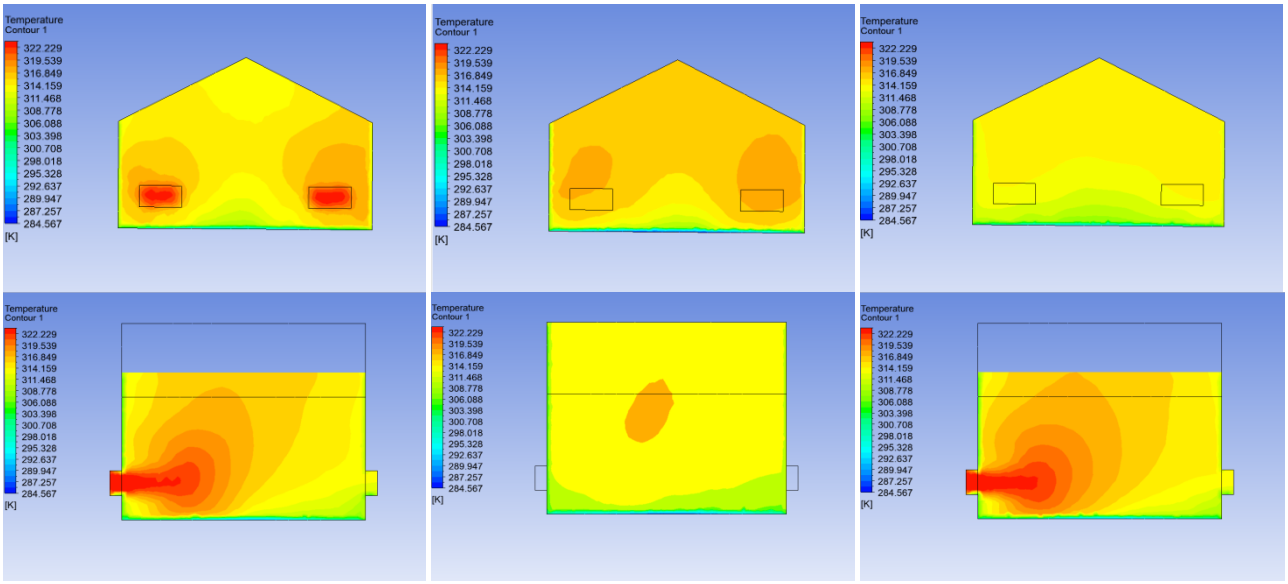

Fig -10: Inside air temperature for the chapel type greenhouse solar dryer; Clockwise from left : Plane A, Plane B, Plane C, Plane D, Plane E, Plane F

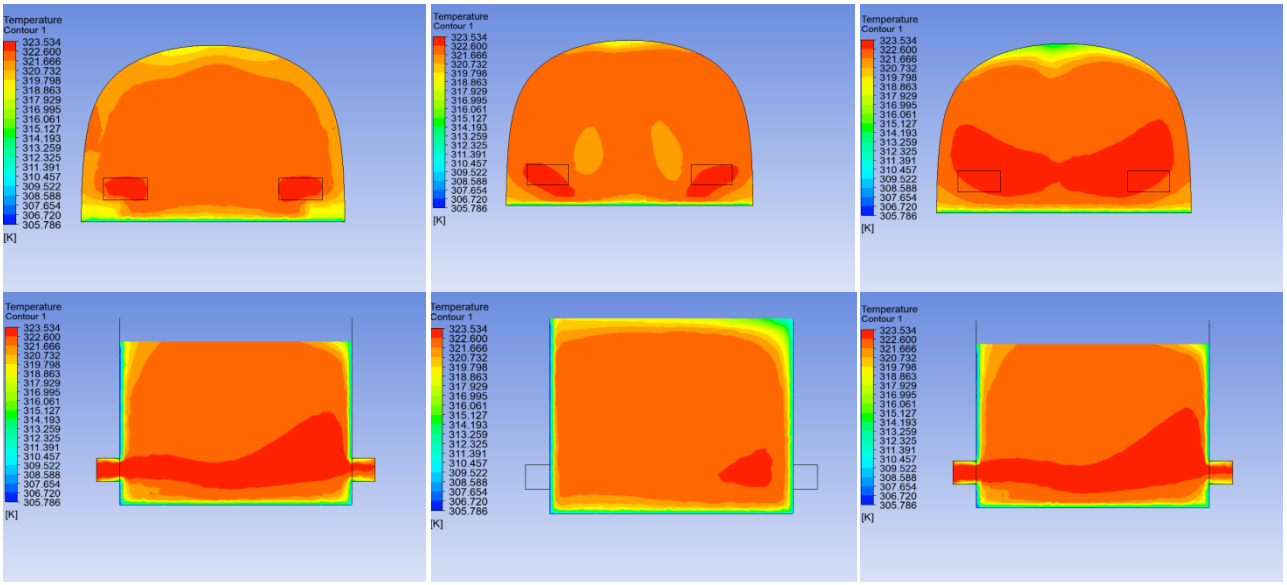

Fig -11: Inside air temperature for the cylindrical roof greenhouse solar dryer; Clockwise from left : Plane A, Plane B, Plane C, Plane D, Plane E, Plane F

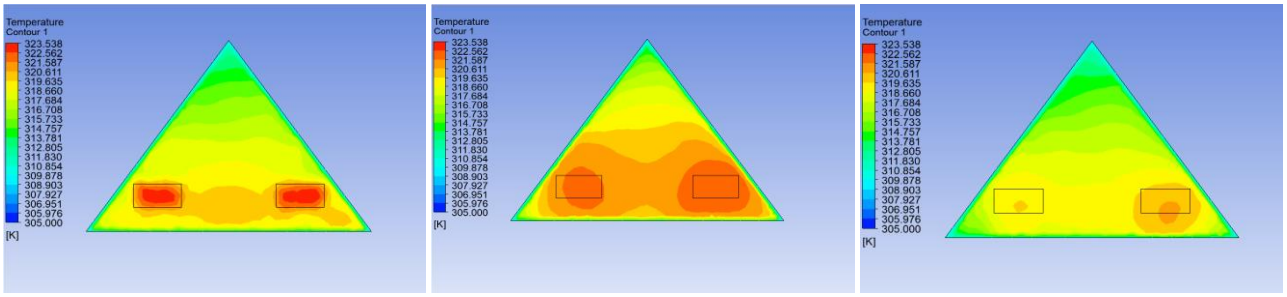

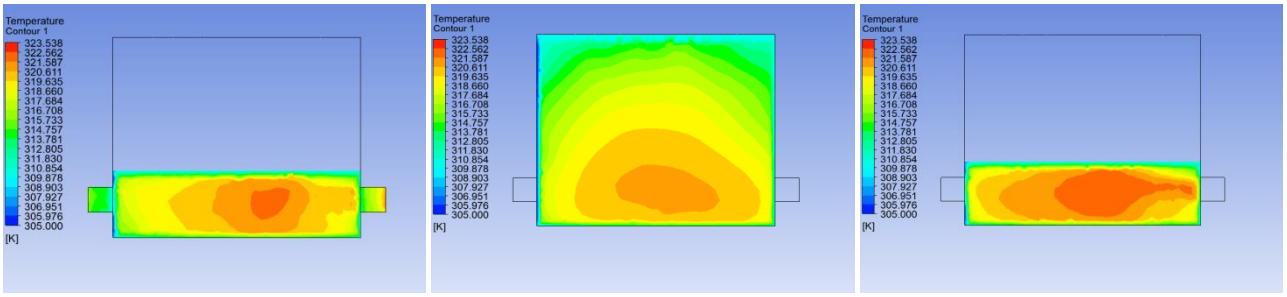

Fig -12: Inside air temperature for the prismatic greenhouse solar dryer; Clockwise from left : Plane A, Plane B, Plane C, Plane D, Plane E, Plane F

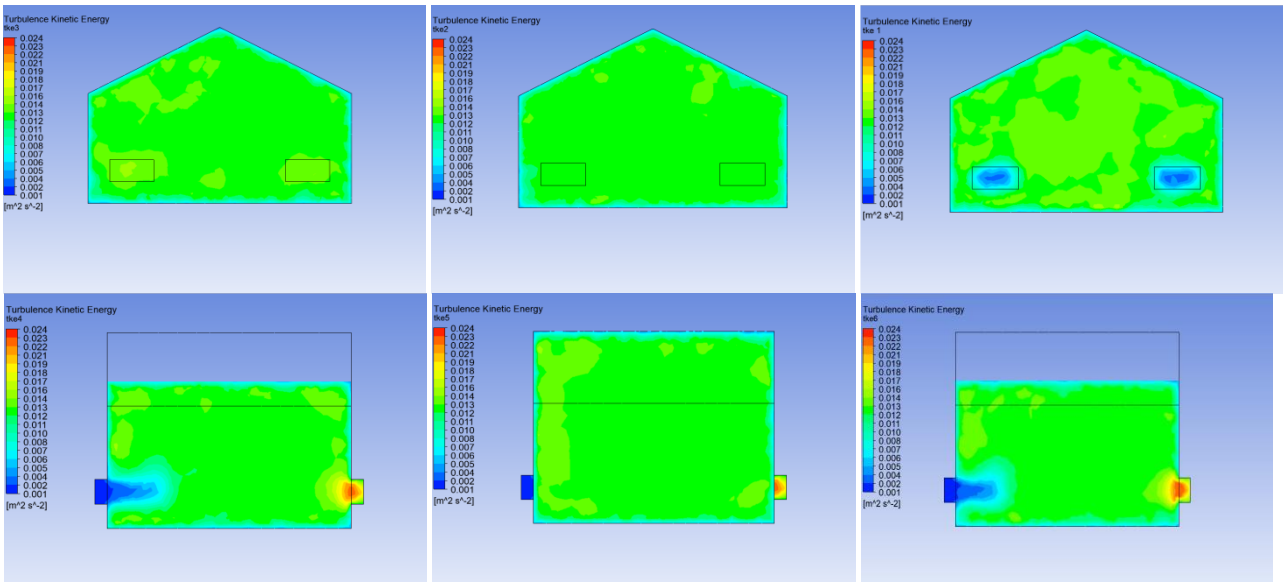

Fig -13: Turbulent kinetic energy for the chapel type greenhouse solar dryer; Clockwise from left : Plane A, Plane B, Plane C, Plane D, Plane E, Plane F

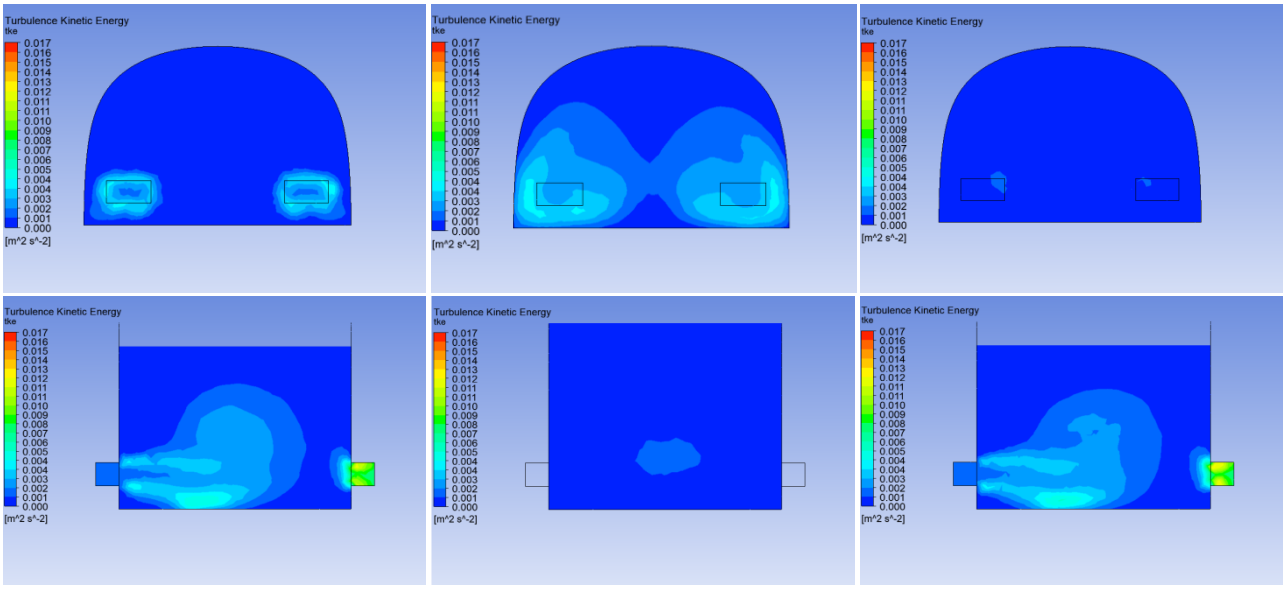

Fig -14: Turbulent kinetic energy for the cylindrical roof greenhouse solar dryer; Clockwise from left : Plane A, Plane B, Plane C, Plane D, Plane E, Plane F

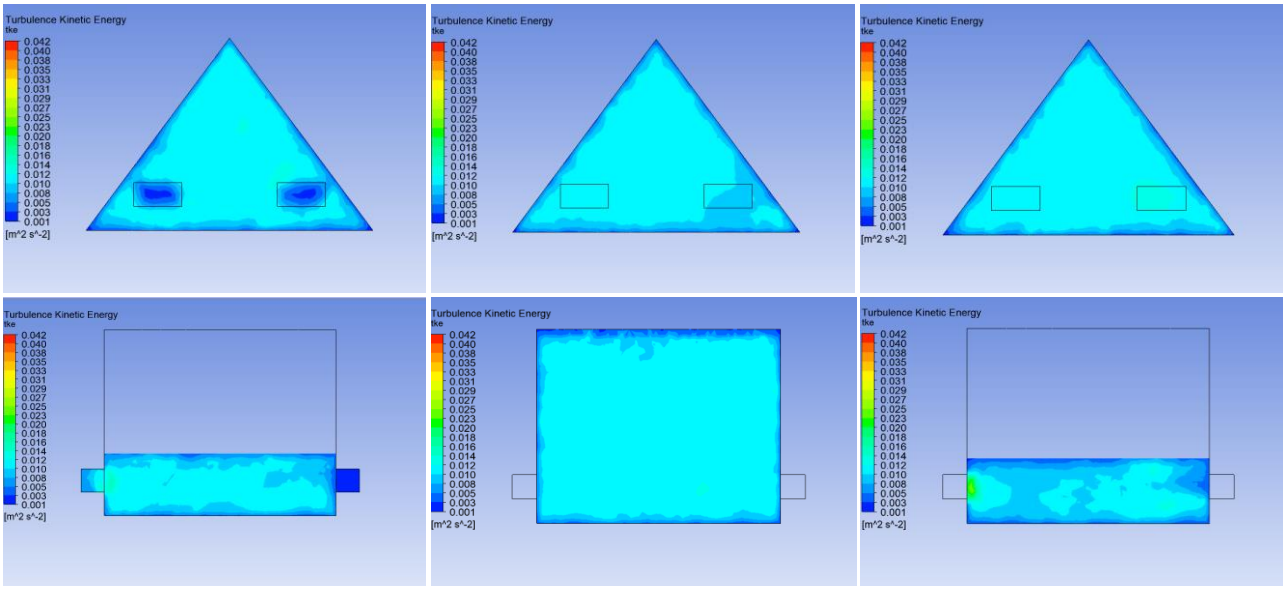

Fig -15: Turbulent kinetic energy for the prismatic greenhouse solar dryer; Clockwise from left : Plane A, Plane B, Plane C, Plane D, Plane E, Plane F

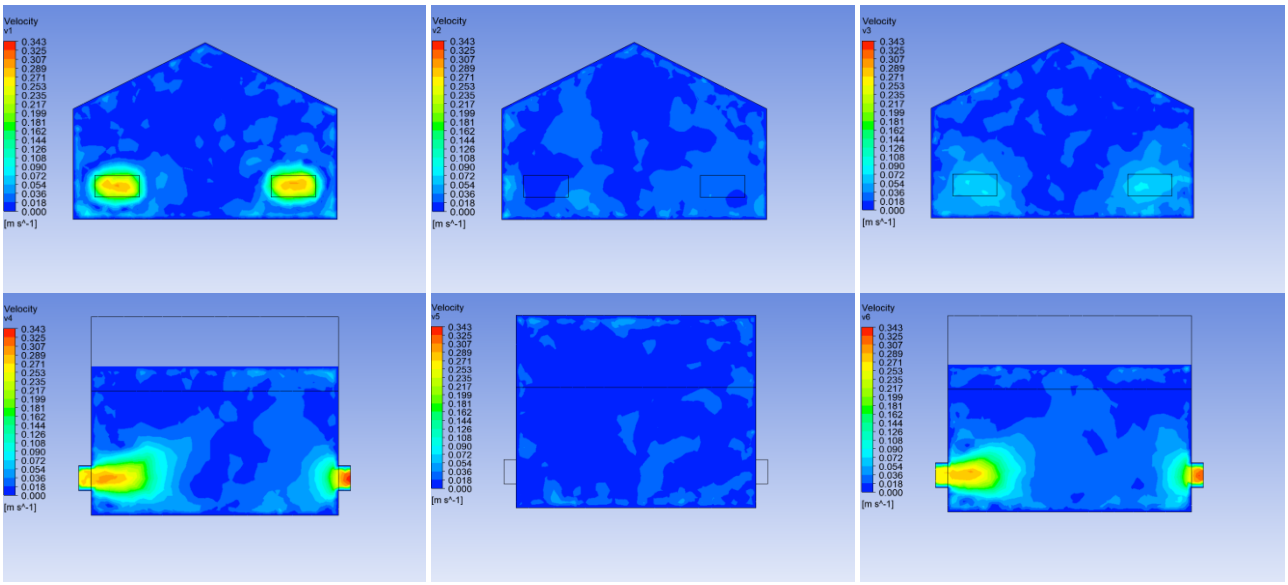

Fig -16: Air velocity for the chapel type greenhouse solar dryer; Clockwise from left : Plane A, Plane B, Plane C, Plane D, Plane E, Plane F

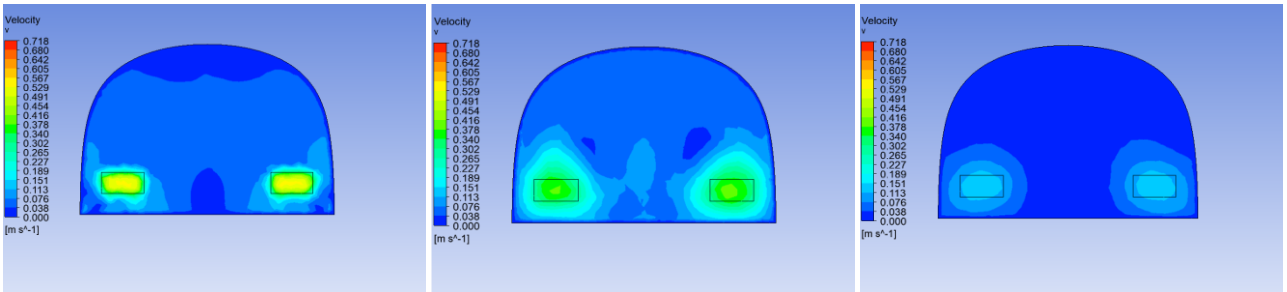

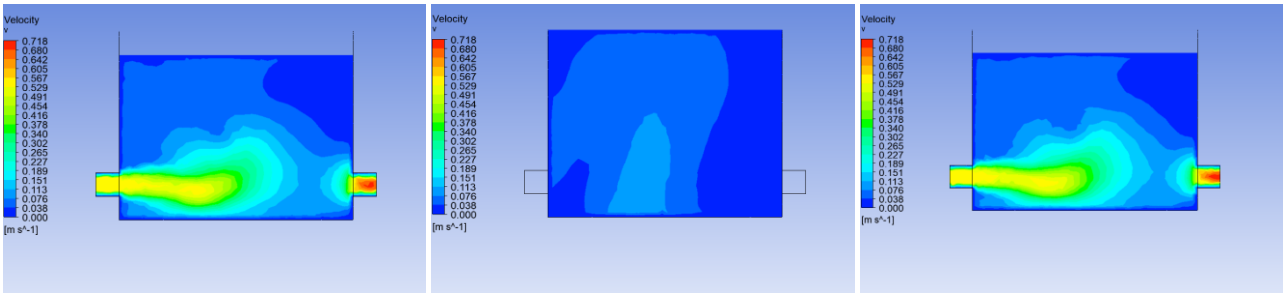

Fig -17: Air velocity for the cylindrical roof greenhouse solar dryer; Clockwise from left : Plane A, Plane B, Plane C, Plane D, Plane E, Plane F

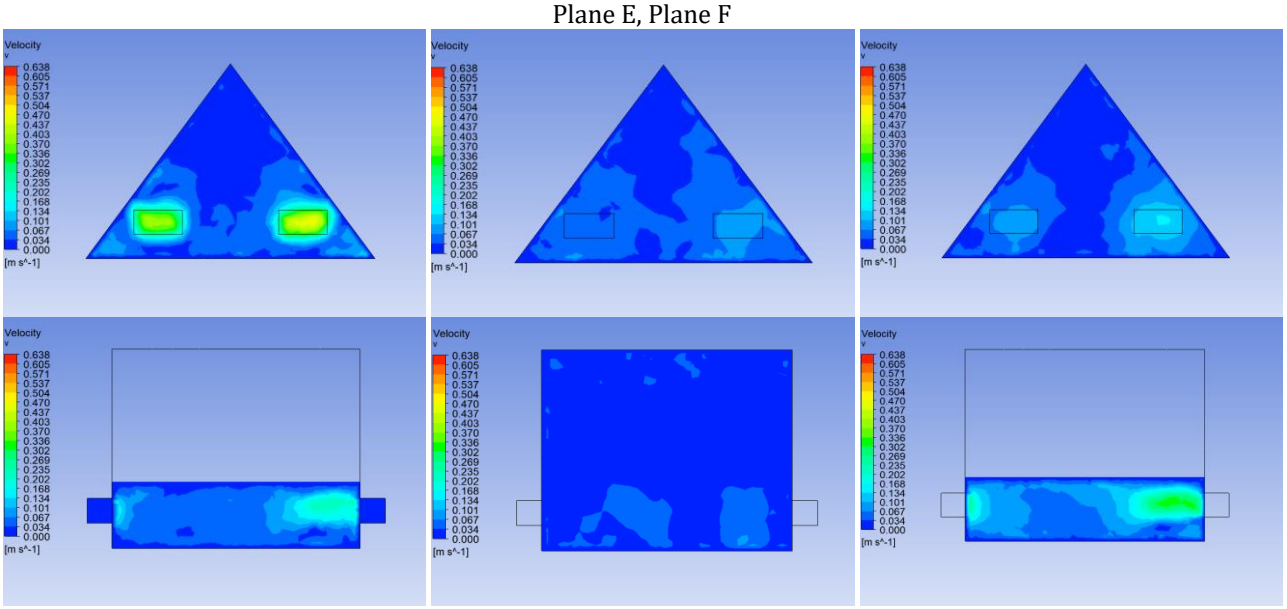

Fig -18: Air velocity for the prismatic greenhouse solar dryer; Clockwise from left : Plane A, Plane B, Plane C, Plane D, Plane E, Plane F

Table -6: Data from different models' parameters

Air temperature [K]	**Minimum**	**Maximum**	**Average**
Chapel type	290	323	314
Cylindrical roof	305	323	321
Prismatic	305	323	317.5
Turbulence Kinetic Energy [m^2/s^2]	**Minimum**	**Maximum**	**Average**
Chapel type	0.001	0.023	0.012
Cylindrical roof	0.001	0.013	0.006
Prismatic	0.001	0.02	0.0095
Air velocity [m/s]	**Minimum**	**Maximum**	**Average**
Chapel type	0	0.3	0.03

Cylindrical roof	0	0.7	0.07
Prismatic	0	0.5	0.045

reduction in intensity as the convective current expands in the space inside. The small sections of planes positioned at angular locations to each other can be held accountable for this observation.

As observed in air temperatures, the graphs of TKE are more homogenous in the chapel type and prismatic greenhouse as opposed to the cylindrical roof greenhouse. Another noteworthy observation is the spike in the average TKE values, which is as much as 0.012 m^2/s^2 for chapel type greenhouse compared to 0.006 m^2/s^2 and 0.0095 m^2/s^2 for the cylindrical roof and prismatic greenhouse, respectively. The maximum values of TKE are obtained for the chapel type model - 0.023 $m^2/s^{2.}$

3.3 Air velocity Results

The humid air velocity profiles are plotted for different models and are displayed in figures 16-18. Higher velocities are noted close to the ground in the case of a cylindrical roof greenhouse, under a height of 1 m. This is important because the rate is related to the drying process' speed[12]. Another spike in air velocities can be noticed near the inlet as well as the outlets. This information can be used to plan the drying substances according to the drying time needs.

The drying rate increased with air velocity for moisture contents above approximately 40% to 50%[14]. The drying rate gradually decreases and tends to level off with air velocities above 3.05 to 3.56 m/s (600 to 700 ft/min) and moisture contents below approximately 80% to 90%. Moreover, the maximum average air velocities are obtained in the cylindrical roof model - 0.07, followed by prismatic and chapel type greenhouse - 0.045 and 0.3. The data is further tabulated in table 6.

4. CONCLUSIONS

This paper sought out to analyze the performance of greenhouse solar dryers using computational fluid dynamics. The parameters used to elucidate the properties were air temperature, turbulence kinetic energy, and air velocity. Different structure geometries were used to compare the effect of greenhouse shape on greenhouse performance characteristics.

The simulation is similar to the research done by Nicolás-Iván Román-Roldán[5] and team. The chapel type greenhouse's physical properties agree with the original readings from the sensors as obtained by the Mexican team. The contours of temperature, air velocity, and turbulent kinetic energy validate the results obtained, and the same procedure is extended to the cylindrical roof and prismatic greenhouse successfully.

The peaks and maximum value of the physical properties vary for different geometries. The maximum average temperature is noted for the cylindrical roof greenhouse, maximum turbulent kinetic energy for the chapel type greenhouse, and the maximum average air velocity for the cylindrical roof greenhouse.

NOMENCLATURE

A0,AS	model constants
C heat	capacity rate, W/K
CP	specific heat at constant pressure, J/(kg·K)
g	gravitational acceleration, m/s2
GSD	greenhouse solar dryer
I	radiative intensity
k	turbulence kinetic energy, m2 /s2
K	conductivity, W/m·K
N degrees	of freedom
P	pressure, Pa
P_b	generation of TKE due to buoyancy
P_k	generation of TKE due to the average velocity
RMSE	root mean square error
S_h	volumetric heat source in the energy equation
S_i source	term due to convection and diffusion
T	temperature, K
TDR	turbulent dissipation rate
TKE	turbulent kinetic energy
t time, s	
V	velocity, m/s
ΔV	volume of the control volume, m3
x	direction, m
YM	fluctuating dilatation in compressible turbulence

SUBSCRIPTS

Exp	experimental
i	coordinate index in x direction
j	coordinate index in
y	direction
k	coordinate index in z direction

GREEK SYMBOLS

ε	dissipation of turbulence energy, m2 /s3
ρ	density, kg/m3
μ	dynamic viscosity, Pa.s

μ_t turbulent viscosity, m2 /s
μ_{ij} coefficient due to convection and diffusion
∇ nabla symbol
λ thermal conductivity, W/(m·K)
κ absorption coefficient
σ scattering coefficient
Ψ viscous dissipation
$\tilde{\Omega}_{ij}$ mean rate of rotation tensor
ω_k angular velocity, m/s

REFERENCES

1. https://www.sciencedirect.com/science/article/abs/pii/S1364032113006242.

2. https://www.researchgate.net/publication/255729204_Analysis_of_Greenhouse_Air_Temperature_Distribution_Using_Geostatistical_Methods.

3. https://www.hindawi.com/journals/psyche/2012/123405/ .

4. https://www.sciencedirect.com/science/article/pii/S1876610219312500

5. https://onlinelibrary.wiley.com/doi/pdf/10.1002/ese3.333

6. Molina-Aiz FD, Valera DL, Álvarez AJ. "Measurement and simulation of climate inside Almerí a-type greenhouses using computational fluid dynamics." Agriculture For Meteorology (2004);125:33–51.

7. Ould Khaoua SA, Bournet PE, Migeon C, Boulard T, Chassériaux G. Analysis of greenhouse ventilation efficiency based on computational fluid dynamics. Biosyst Eng. 2006;95:83-98.

8. https://www.afs.enea.it/project/neptunius/docs/fluent/html/th/node115.htm#:~:text=The%20DO%20model%20allows%20you,scattering%20in%20the%20gas%20phase.&text=%2C%20defined%20in%20Equation%205.3%2D13,used%20in%20the%20scattering%20terms.

9. FLUENT 12.1 User's Guide, Fluent Inc. Available online: http:// www.afs.enea.it/project/neptunius/docs/fluent; 2018.

10. Favre A. Equations des gaz turbulents compressibles. J Mec. 1965;3:361-390.

11. Ould Khaoua SA, Bournet PE, Migeon C, Boulard T, Chassériaux G. Analysis of greenhouse ventilation efficiency based on computational fluid dynamics. Biosyst Eng. 2006;95:83-98.

12. Velić D, Planinić M, Tomas S, Bilic M. Influence of airflow velocity on kinetics of convection apple drying. J Food Eng. 2004;64:97-102.

13. www.greenhousemanagement.com/greenhouse_management/managing_temperature_greenhouse_crops/temperature_requirements_greenhouse_crops.htm

14. https://www.fpl.fs.fed.us/documnts/fplrn/fplrn266.pdf#:~:text=The%20drying%20rate%20increased%20with,approximately%2080%25%20to%2090%25